

# Nanoparticles of $\beta$ -Cyclodextrin Esters Obtained by Self-Assembling of Biotransesterified $\beta$ -Cyclodextrins

Luc Choisnard,\*<sup>†</sup> Annabelle Gèze,<sup>†</sup> Jean-Luc Putaux,<sup>‡</sup> Yung-Sing Wong,<sup>†</sup> and Denis Wouessidjewe<sup>†</sup>

Université Joseph Fourier, UFR de Pharmacie, ICMG DPM UMR CNRS 5063, 5 Avenue de Verdun, F-38243 Meylan Cedex, France, and Centre de Recherches sur les Macromolécules Végétales, ICMG, UPR CNRS 5301, BP 53, F-38041 Grenoble Cedex 9, France

Received October 12, 2005; Revised Manuscript Received November 30, 2005

The synthesis of decanoate  $\beta$ -cyclodextrin esters ( $\beta$ -CDd) and hexanoate  $\beta$ -cyclodextrin esters ( $\beta$ -CDh) was biocatalyzed by thermolysin from native  $\beta$ -cyclodextrin ( $\beta$ -CD) and vinyl hexanoate or vinyl decanoate used as acyl donors. The products were chemically characterized by infrared, NMR, and mass spectrometry. Both  $\beta$ -CDd and  $\beta$ -CDh esters were identified as a mixture of  $\beta$ -CD preferentially substituted on the C2 position by the corresponding acyl chain. The degree of substitution varied from 2 to 7 for  $\beta$ -CDd and from 4 to 8 for  $\beta$ -CDh. The ability of  $\beta$ -CD esters to self-organize into nanoparticles was tested using a nanoprecipitation technique in various solvents. The mean size diameter and polydispersity measured by quasi-elastic light scattering were dramatically affected by the nature of solvent (acetone, ethanol, or tetrahydrofuran) used in the nanoprecipitation technique. When directly observed using cryo-transmission electron microscopy,  $\beta$ -CDh appeared as uniformly dense nanospheres, whereas  $\beta$ -CDd exhibited a multilamellar onion-like organization. A structural model was rationalized for the  $\beta$ -CDd nanoparticles.

## Introduction

Cyclodextrins (CD) are well-known cyclic oligosaccharides which are manufactured by glucosyltransferase degradation of starch. The classical cyclodextrin series are constituted of six ( $\alpha$ -CD), seven ( $\beta$ -CD), or eight ( $\gamma$ -CD) D-glucopyranoside units linked by  $\alpha$ -1,4 bonds.<sup>1</sup> One of the most remarkable features of the CD is their ability to incorporate small hydrophobic molecules in their cavity. This molecular encapsulation confers to the complex formed some different physicochemical properties compared to those of the guest molecule alone. For example, the bioavailability of several poorly water soluble pharmaceutically active compounds can be improved using CD as a molecular carrier.<sup>2</sup> The earliest reference reporting the use of CD in drug formulation was published in 1953.<sup>3</sup> From this date, the use of CDs in pharmaceutical applications was continually raised and generalized.

In the past decade, considerable interest has been shown in the development of new vectors based on different hydrophobic CD derivatives. These macrocyclic amphiphiles can form a variety of supramolecular assemblies, such as micelles,<sup>4,5</sup> vesicles,<sup>6,7</sup> and nanoparticles.<sup>8–10</sup> In this area, amphiphilic  $\beta$ -cyclodextrins obtained by grafting aliphatic chains on the primary or secondary face exhibit self-organization properties yielding stable nanospheres or nanocapsules.<sup>11–15</sup> A good knowledge of the nanoaggregate ultrastructure is essential to the development of drug carriers. It is worth reminding that the ability to encapsulate drugs is partly related to the internal structure of nanosystems.

Regioselectively acylated  $\beta$ -CD on the secondary hydroxyl groups are typically synthesized in a three-step procedure from

the  $\beta$ -CD: (i) protection of primary hydroxyl groups, (ii) acylation of the secondary face, (iii) deprotection of primary face.<sup>16</sup> However, the use of enzymes allowing a one-step catalysis in organic solvent with low water content appears to be an interesting alternative pathway. Indeed, the biocatalyzed production of carbohydrate esters has already been efficiently undertaken in the past.<sup>17–19</sup> CD acylation has been achieved using proteinase N, subtilisin, or lipase.<sup>20–22</sup> More recently, Pedersen et al.<sup>23</sup> developed a very efficient one-step-catalyzed transesterification of various cyclodextrins by vinyl–acyl fatty esters in the presence of thermolysin.

The present work describes the preparation of nanoparticles made of decanoate  $\beta$ -CD ester ( $\beta$ -CDd) and hexanoate  $\beta$ -CD ester ( $\beta$ -CDh) obtained by a thermolysin-catalyzed acylation of  $\beta$ -CD with vinyl decanoate and vinyl hexanoate as acyl donors. Both  $\beta$ -CD esters were characterized by infrared, NMR, and mass spectrometry. The ability of the derivatives to self-assemble was evaluated. The influence of formulation conditions on the mean size of particles was studied. Cryo-transmission electron microscopy (cryo-TEM) revealed the existence of particles displaying original morphologies never observed with acylated cyclodextrins. A model of the ultrastructure for  $\beta$ -CDh-based nanoparticles is presented.

## Experimental Section

**Materials.** Thermolysin (EC 3.4.24.27), a protease type X isolated from *Bacillus thermoproteolyticus* rokko, anhydrous DMSO (99%), vinyl decanoate (95%), and Celite were obtained from Sigma Aldrich (Sigma Aldrich, L'Isle D'Abeau Chesnes, France). Vinyl hexanoate (99%) was purchased from TCI Europe nv (Interchim, Montluçon, France).  $\beta$ -CD (Kleptose) was donated by Roquette (Roquette, Lestrem, France). Anhydrous acetone, ethanol, and tetrahydrofuran (THF) were from VWR (VWR International, Lyon, France). Water was freshly deionized in our laboratory.

\* Corresponding author. Phone: (33) 04 76 04 10 01. Fax: (33) 04 76 04 10 12. E-mail: luc.choisnard@ujf-grenoble.fr.

<sup>†</sup> Université Joseph Fourier.

<sup>‡</sup> Centre de Recherches sur les Macromolécules Végétales.

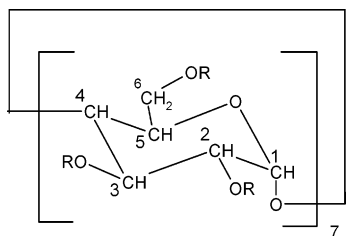


**Figure 1.** Schematic  $\beta$ -CD esters structure: R = H or  $-\text{CO}-(\text{CH}_2)_8-\text{CH}_3$  for the decanoate  $\beta$ -CD ester or  $-\text{CO}-(\text{CH}_2)_4-\text{CH}_3$  for the hexanoate  $\beta$ -CD ester according to the degree of substitution and the distribution of the functional group on the  $\beta$ -CD backbone.

**Enzyme Immobilization.** Celite (10 g) was regenerated by stirring for 6 h at 80 °C in 100 mL of nitric acid 69%. Then, the acid was removed by filtration, and the Celite was washed with deionized water ( $10 \times 100$  mL) until a stable pH = 6.5 was reached. The resulting wet Celite was dried under reduced pressure and stored overnight at 100 °C. Thermolysin (100 mg) was mixed in 5 mL of MOPS/Na buffer (50 mM, pH = 7.5) at 20 °C. The obtained preparation was added with 1 g of the regenerated Celite and maintained under stirring for 4 h. The liquid phase of this preparation was removed at 25 °C under reduced pressure to yield the immobilized thermolysin which was immediately used.

**Synthesis of Decanoate and Hexanoate  $\beta$ -Cyclodextrin Esters.** Biocatalyzed acylation of  $\beta$ -CD and purification of the  $\beta$ -CD esters synthesized were achieved using a modified procedure developed by Pedersen et al.<sup>23</sup>  $\beta$ -CD was dried under reduced pressure (1 mbar) for 48 h at 80 °C in the presence of  $\text{P}_2\text{O}_5$ . Then, the dried  $\beta$ -CD (1 g; 881  $\mu\text{moles}$ ) was solubilized in DMSO (7.5 mL) and mixed with the Celite-immobilized thermolysin (1.1 mg). The temperature of the mixture under stirring (250 rpm) was raised to 45 °C.

Then, vinyl decanoate (2.5 mL; 10.6 mmol) or vinyl hexanoate (1.6 mL; 10.6 mmol) was introduced in the suspension in order to start the esterification which lasted 70 h. At the end of the reaction, the immobilized thermolysin was removed from the liquid phase by centrifugation (150 000 rpm; 15 min). The  $\beta$ -CD esters in the supernatant were precipitated by adding 20 mL of MeOH/H<sub>2</sub>O (35/65; v/v). The crude product was washed twice with 10 mL of a DMSO/MeOH/H<sub>2</sub>O (50/35/65; v/v/v) mixture. In the case of  $\beta$ -CDd synthesis, the residues of vinyl decanoate and DMSO were removed using flash chromatography with  $\text{CH}_3\text{Cl}/\text{MeOH}$  (95/5; v/v) and  $\text{CH}_3\text{Cl}/\text{MeOH}$  (50/50; v/v) as mobile phases. In the case of  $\beta$ -CDh esters synthesis, the unreacted vinyl hexanoate and residual DMSO were removed using flash chromatography with  $\text{CH}_2\text{Cl}_2/\text{MeOH}$  (90/10; v/v) and  $\text{CH}_2\text{Cl}_2/\text{MeOH}$  (5/95; v/v) as mobile phases.  $\beta$ -CD ester was dried under reduced pressure.

Infrared spectra were measured from KBr pellets using a Bruker Vector 22 spectrophotometer (Bruker, Germany). NMR spectra were recorded on a BRUKER 400 ULTRASHIELD (Bruker, Germany).  $\beta$ -CD esters were also analyzed by MALDI-TOF MS on the BRUKER AUTOFLEX apparatus (Bruker, Germany). Ester (1 mg) was solubilized in a minimum volume of MeOH. This solution was mixed in the same proportion with trifluoroacetic acid 0.1% (v/v) in  $\text{CH}_3\text{CN}$  33% saturated with  $\gamma$ -cyano-4-hydroxy cinnamic acid. Then, 1  $\mu\text{L}$  of the subsequent solution was applied to the target plate (DHB).

The  $\beta$ -CDd ester (0.92 g) was obtained as a white powder (see the theoretical chemical structure in Figure 1). IR (KBr):  $\nu$  ( $\text{cm}^{-1}$ ) = 3428 (OH), 1741 ( $\text{CO}_{\text{ester}}$ ), 2918 ( $-\text{CH}-$ ).  $^1\text{H}$  NMR (400 MHz; DMSO- $d_6$ ):  $\delta$  (ppm) = 0.85 ( $-\text{CH}_2-\text{CH}_2-(\text{CH}_2)_6-\text{CH}_3$ ), 1.24 ( $-\text{CH}_2-\text{CH}_2-(\text{CH}_2)_6-\text{CH}_3$ ), 1.52 ( $-\text{CH}_2-\text{CH}_2-(\text{CH}_2)_6-\text{CH}_3$ ), 2.32 ( $-\text{CH}_2-\text{CH}_2-(\text{CH}_2)_6-\text{CH}_3$ ), 3.45 (H-4), 3.60 (H-5, H-6), 3.76 (H-3, H-6'), 4.43 (H-2), 4.61 (OH-3, OH-6), 5.06 (H-1).  $^{13}\text{C}$  NMR (100 MHz; DMSO- $d_6$ ):  $\delta$  (ppm) = 14.4 ( $-\text{CH}_2-\text{CH}_2-(\text{CH}_2)_6-\text{CH}_3$ ), 24.7 ( $-\text{CH}_2-\text{CH}_2-(\text{CH}_2)_6-\text{CH}_3$ ), 26.2, 29.2, and 31.8 ( $-\text{CH}_2-\text{CH}_2-(\text{CH}_2)_6-\text{CH}_3$ ), 33.9 ( $-\text{CH}_2-\text{CH}_2-(\text{CH}_2)_6-\text{CH}_3$ ), 60.3 (C-6), 69.8 (C-3), 72.2 (C-5), 73.5 (C-2), 80.6 (C-4), 98.0 (C-1), 173.4 ( $-\text{CO}-$ ). MALDI-MS:  $m/z$  =

1465.5 (relative intensity, 24%) [decanoate  $\beta$ -CD ester with 2 chains +  $\text{Na}^+$ ], 1619.7 (relative intensity, 80%) [decanoate  $\beta$ -CD ester with 3 chains +  $\text{Na}^+$ ], 1773.8 (relative intensity, 100%) [decanoate  $\beta$ -CD ester with 4 chains +  $\text{Na}^+$ ], 1928.0 (relative intensity, 83%) [decanoate  $\beta$ -CD ester with 5 chains +  $\text{Na}^+$ ], 2082.1 (relative intensity, 37%) [decanoate  $\beta$ -CD ester with 6 chains +  $\text{Na}^+$ ], 2236.2 (relative intensity, 8%) [decanoate  $\beta$ -CD ester with 7 chains +  $\text{Na}^+$ ].

The  $\beta$ -CDh ester (0.98 g) was also isolated as a white powder (Figure 1). IR (KBr):  $\nu$  ( $\text{cm}^{-1}$ ) = 3426 (OH), 1740 ( $\text{CO}_{\text{ester}}$ ), 2918 ( $-\text{CH}-$ ).  $^1\text{H}$  NMR (400 MHz; DMSO- $d_6$ ):  $\delta$  (ppm) = 0.85 ( $-\text{CH}_2-\text{CH}_2-(\text{CH}_2)_2-\text{CH}_3$ ), 1.27 ( $-\text{CH}_2-\text{CH}_2-(\text{CH}_2)_2-\text{CH}_3$ ), 1.54 ( $-\text{CH}_2-\text{CH}_2-(\text{CH}_2)_2-\text{CH}_3$ ), 2.32 ( $-\text{CH}_2-\text{CH}_2-(\text{CH}_2)_2-\text{CH}_3$ ), 3.39 (H-4), 3.60 (H-5, H-6), 3.75 (H-3, H-6'), 4.44 (H-2), 4.62 (OH-3, OH-6), 5.06 (H-1).  $^{13}\text{C}$  NMR (100 MHz; DMSO- $d_6$ ):  $\delta$  (ppm) = 14.3 ( $-\text{CH}_2-\text{CH}_2-(\text{CH}_2)_2-\text{CH}_3$ ), 22.3 and 31.1 ( $-\text{CH}_2-\text{CH}_2-(\text{CH}_2)_2-\text{CH}_3$ ), 24.4 ( $-\text{CH}_2-\text{CH}_2-(\text{CH}_2)_2-\text{CH}_3$ ), 33.9 ( $-\text{CH}_2-\text{CH}_2-(\text{CH}_2)_2-\text{CH}_3$ ), 60.3 (C-6), 69.8 (C-3), 72.3 (C-5), 73.25 (C-2), 80.4 (C-4), 97.9 (C-1), 173.4 ( $-\text{CO}-$ ). MALDI-MS:  $m/z$  = 1549.6 (relative intensity, 3%) [hexanoate  $\beta$ -CD ester with 4 chains +  $\text{Na}^+$ ], 1647.6 (relative intensity, 56%) [hexanoate  $\beta$ -CD ester with 5 chains +  $\text{Na}^+$ ], 1745.7 (relative intensity, 100%) [hexanoate  $\beta$ -CD ester with 6 chains +  $\text{Na}^+$ ], 1844.8 (relative intensity, 60%) [hexanoate  $\beta$ -CD ester with 7 chains +  $\text{Na}^+$ ], 1941.8 (relative intensity, 3%) [hexanoate  $\beta$ -CD ester with 8 chains +  $\text{Na}^+$ ].

**Nanoparticle Preparation.** The nanoparticle suspensions were prepared using the nanoprecipitation technique.<sup>12</sup> An amount of 10 mg of  $\beta$ -CDd product was dissolved at 25 °C in 10 mL of acetone, ethanol, or THF and poured slowly through a silicon tube fitted with fine tip into distilled water (10 mL) subjected to a magnetic stirring. The nanospheres were formed immediately, and the colloidal suspension obtained was submitted to evaporation under reduced pressure to remove the organic solvent. The resulting colloidal suspension was filtered through a 0.8  $\mu\text{m}$  membrane (Millex AA, Millipore, France) and stored in closed vials at room temperature. A nanosphere suspension was also prepared with the same procedure from  $\beta$ -CDh (20 mg) first solubilized in 10 mL of acetone, ethanol, or THF and poured into 20 mL of water.

**Particle Size Measurements.** The size of freshly made nanoparticles in water suspension was measured in triplicate by quasi-elastic light scattering (QELS) using a Zetasizer 3000 instrument (10 mW HeNe laser at 632.8 nm, K7132 correlator, Malvern). The experimental conditions were the following: temperature  $25 \pm 0.1$  °C, reference angle 90°, viscosity  $0.899 \times 10^{-3}$  Pa·s, refractive index 1.330. The polydispersity index (PI), which is a dimensionless measure of the broadness of the size distribution, and Z-average mean hydrodynamic diameter (Dh) of the particles were calculated using a Contin algorithm with Zetasizer 3000 software version V. 1.51 automatic Contin.<sup>24</sup> Dh values were derived from the measured translational diffusion coefficient of particles moving under Brownian motion.

**Transmission Electron Microscopy.** According to the procedure described elsewhere,<sup>25</sup> specimens for cryo-TEM were prepared by quench-freezing thin liquid films of 3 mg/mL (w/v)  $\beta$ -CD ester suspensions into liquefied ethane ( $-171$  °C). Once transferred in a Gatan 626 cryoholder cooled with liquid nitrogen, the specimens were observed at low temperature ( $-180$  °C), using a Philips CM200 "Cryo" microscope operating at 80 kV. The low-dose procedure (Philips) was used to prevent any detrimental radiation damage in the areas of interest before actual image recording on Kodak SO163 films.

## Results and Discussion

**$\beta$ -CD Esters Synthesis.** The esterification of  $\beta$ -CD was not observed in the "control media" containing only regenerated Celite without thermolysin. On the other hand, in the presence of thermolysin immobilized by deposition on Celite, a mixture of variously acylated  $\beta$ -CD was obtained with both acyl donors.

The NMR spectra of the  $\beta$ -CDh esters were assigned by comparison with the corresponding spectra of native  $\beta$ -CD and

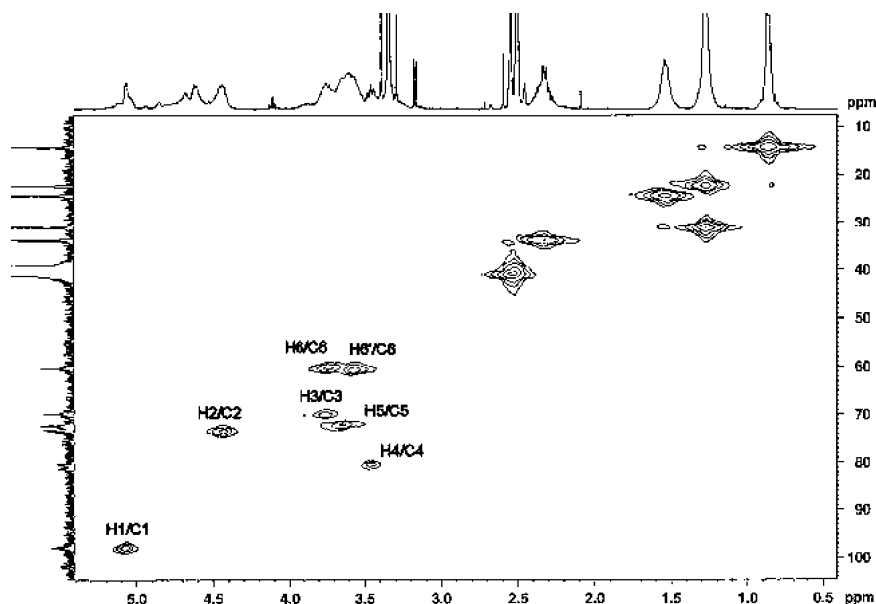


**Figure 2.** HMQC NMR spectrum for the hexanoate  $\beta$ -CD ester mixture.

vinyl hexanoate precursors. Then, for the native  $\beta$ -CD, the proton signal of the 2-OH secondary hydroxyl groups observed by  $^1\text{H}$  NMR analysis was measured with a chemical shift at  $\delta = 5.65$  ppm. In contrast, for the  $\beta$ -CDh ester product, the corresponding signal was not observed in this region because the 2-OH groups greatly reacted with vinyl hexanoate. Supporting this observation, the heteronuclear multiple-quantum coherence (HMQC) spectrum of the hexanoate  $\beta$ -CD ester did not show any shift of correlation between the resonance peaks of H3/C3 and H6/C6 (Figure 2). This means that the formation of product substituted at the C3 and C6 position was not detected.

It was concluded that the thermolysin esterification of native  $\beta$ -CD by vinyl hexanoate mainly occurred at the C2 position and the substitutions on C3 and C6 position should be marginal. The MALDI-TOF analysis of the  $\beta$ -CDh product showed a group of signals sequentially separated by 99 mass units which correspond to the molecular mass of the hexanoate chain unit. This result indicates the presence of the  $\beta$ -CDh mixture constituted by  $\beta$ -CD with a variable degree of substitution ranging from 4 to 8 hexanoate units ( $m/z$ , 1549.6–1941.8).

The  $^1\text{H}$  and  $^{13}\text{C}$  NMR attributions of the  $\beta$ -CDd esters were in accordance with those observed by Pedersen et al.<sup>23</sup> for the same product. However, in the present work, the MALDI-TOF analysis of the  $\beta$ -CDd esters showed the existence of a mixture of species with only 3–7 substitutions ( $m/z$ , 1465.5–2236.2). This product was slightly underesterified in comparison with Pedersen's product which was 6–9-acylated. This difference between the reaction yields may be partially due to a divergence of the synthesis procedure and to the specific activity of the thermolysin used (Calbiochem-Novabiochem Corp., Meudon, France vs Sigma Aldrich, L'Isle D'Abeau Chesnes, France).

**$\beta$ -CD Esters Self-Organization.** The ability of the deca- and hexanoate  $\beta$ -CD esters to self-organize has been evaluated in the conditions of the solvent displacement procedure. Each amphiphilic derivative previously dissolved in organic solvent formed nanometric particles when in contact with a required amount of water. The formulation conditions were selected in order to induce the immediate desolvation of the  $\beta$ -CD ester following contact with the water phase. Thus, the experimental conditions of nanoprecipitation were adapted for each derivative. As a consequence, the mass concentration of the organic phase

**Table 1.** Mean Hydrodynamic Diameters and Polydispersity Indexes (PI) of  $\beta$ -CDh and  $\beta$ -CDd Nanoparticles Prepared Using Acetone, Ethanol, or Tetrahydrofuran

	acetone		ethanol		tetrahydrofuran	
	mean size diameter (nm)	PI	mean size diameter (nm)	PI	mean size diameter (nm)	PI
$\beta$ -CDh	275.1	0.05	291.5	0.03	293.2	0.05
$\beta$ -CDd	160.9	0.01	219.3	0.03	326.4	0.17

containing  $\beta$ -CDh was twice the one for  $\beta$ -CDd. The amount of aqueous phase was also higher. This behavior may result from the difference in solubility of the derivatives in the organic solvents considered in the study. A deeper physicochemical characterization of both derivatives is being carried out in order to elucidate this point.

Since the desolvation step is induced by reciprocal diffusion of organic solvent in water, the influence of the nature of the organic solvent used in the procedure on the final suspension characteristics was investigated using either acetone, ethanol, or THF. These solvents were selected for their water miscibility and low toxic potential (class III solvents).<sup>26</sup> It clearly appeared that the use of either acetone or ethanol yielded stable nanoparticle suspensions presenting the Tyndall effect, characteristic of the colloidal state. In these cases, no flocculation was observed with either decanoate or  $\beta$ -CDh esters. At the opposite, the experiments involving the decanoate or hexanoate derivative performed in the presence of THF led to nanosuspensions which tended to flocculate. It has to be noted that in this case an important amount of  $\beta$ -CD ester initially introduced in the formulation precipitated and was lost during the filtration step.

Table 1 gives the values of mean hydrodynamic diameters of nanoparticles from each suspension. Mean sizes between 160 and 330 nm were observed, depending on the experimental conditions. As a result, the use of acetone in the organic phase allowed us to obtain monodisperse suspensions of nanoparticles presenting a mean size lower than that of particles obtained when ethanol was used. This tendency was observed for both derivatives. Size deviations of 60 and 20 nm were observed for  $\beta$ -CDd and  $\beta$ -CDh, respectively, in nanosuspensions prepared from acetone and ethanol, respectively. This point is in agreement with previous results obtained in the case of amphiphilic  $\beta$ -CD chemically modified<sup>16</sup> with alkyl chains on the secondary face, which are well-known to self-assemble and



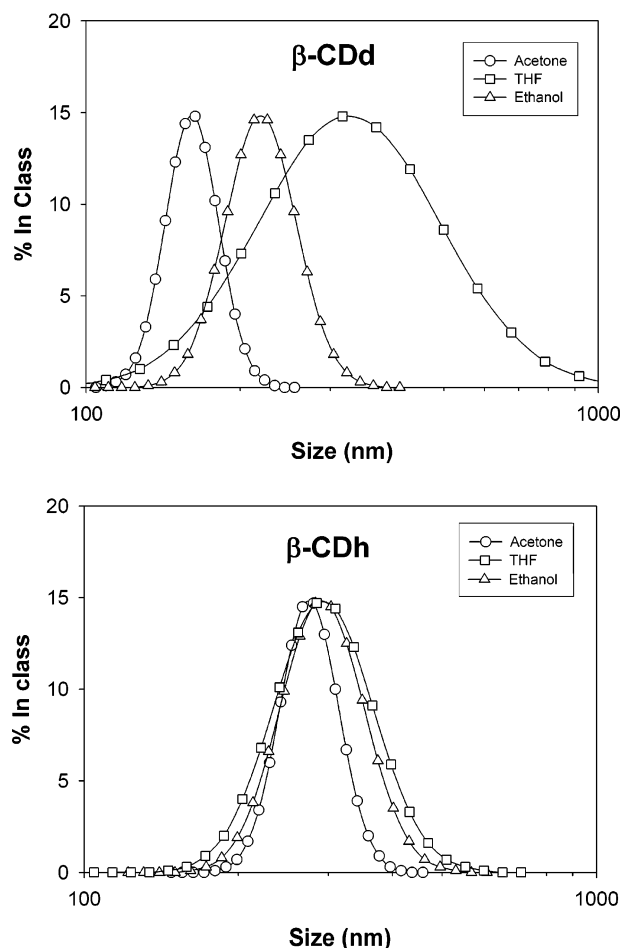


**Figure 3.** Quasi-elastic light scattering size distribution of  $\beta$ -CDh- and  $\beta$ -CDd-based nanoparticles.

form aqueous suspensions of nanospheres, in conditions of nanoprecipitation. Indeed, the mean size of amphiphilic  $\beta$ -CD-based nanospheres could be easily controlled in the range of 60–400 nm by varying the solvent ratios (acetone/ethanol/water) involved in the process.<sup>27</sup>

Besides a higher particle mean size (293 and 326 nm for  $\beta$ -CDh and  $\beta$ -CDd, respectively), the formulations involving the use of THF presented a larger distribution, more pronounced in the case of the decanoate derivative, as revealed by the polydispersity index (PI) value close to 0.2 (Figure 3). This result was in agreement with the nanosuspension instability observed after nanoprecipitation. Consequently, THF was not adapted in these experimental conditions.

**Cryo-Electron Microscopy Observations.** Thin vitrified films of  $\beta$ -CDh and  $\beta$ -CDd nanosystems prepared with acetone as the organic phase were observed using cryo-TEM.

Figure 4 shows a typical image of the  $\beta$ -CDh preparation. Individual spherical particles can be seen. They are rather polydisperse. Their diameter ranges from 50 to 300 nm with an average value of 260 nm estimated from several micrographs were in good agreement with the mean size measured using light scattering (Table 1). The objects appeared to be uniformly dense, and no particular structure was detected in the images. The aspect of these particles was similar to that of amphiphilic  $\beta$ -CD prepared using a three-step chemical synthesis.<sup>15</sup>

The particles prepared from  $\beta$ -CDd also appeared to be spherical. However, they were smaller than those prepared from  $\beta$ -CDh and less polydisperse (Figure 5a).

Their diameters ranged from 80 to 150 nm with an average value of 130 nm. A few rectangular objects were observed

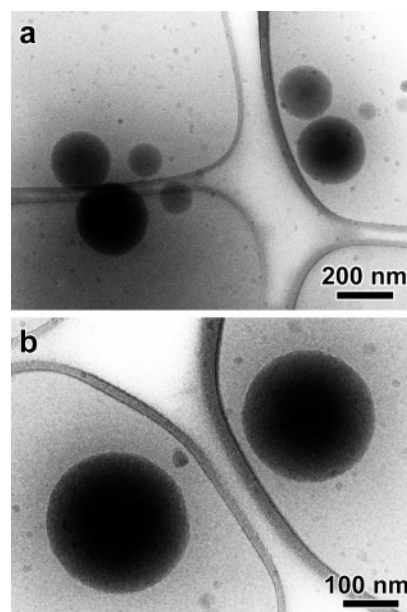


**Figure 4.** Cryo-TEM images of  $\beta$ -CDh nanoparticles embedded in vitreous ice.

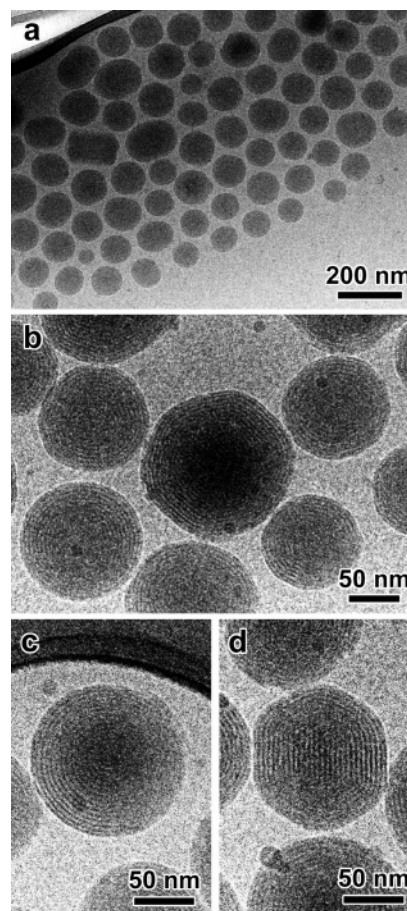


**Figure 5.** Cryo-TEM images of  $\beta$ -CDd nanoparticles embedded in vitreous ice: (a) general view; (b) multilamellar structure visible at higher magnification; (c) a particle entirely made of concentric layers; (d) a polygonal particle with a crystal-like core surrounded by a shell of concentric layers.

suggesting that some particles may be barrel-shaped (Figure 5a). One may argue that most particles in the images may correspond to transverse views of barrel-shaped objects. However, considering the typical thickness of the vitreous ice films prepared for cryo-TEM (80–150 nm) and the length of the elongated

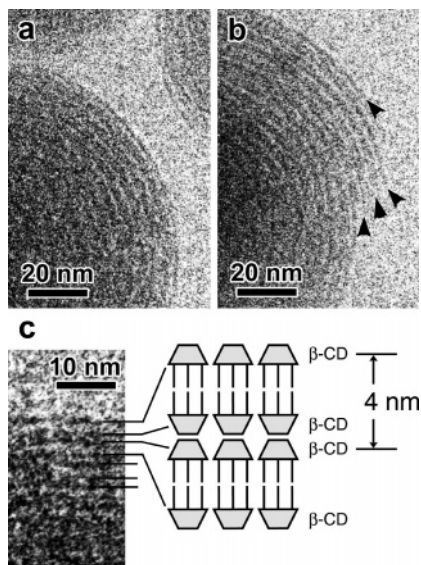


**Figure 6.** (a, b) Details of the bilayer organization at the periphery of selected nanospheres (cryo-TEM images); (c) tentative model describing the organization of amphiphilic  $\beta$ -CDd molecules into bilayers.

particles, we assumed that statistically, barrel-shaped objects would orient longitudinally in the embedded liquid film and not with their long axis parallel to the electron beam. The occurrence of rectangular particles in the distributions being rather rare, we considered that they were not statistically significant.

When imaged at higher magnification (Figure 5b), the  $\beta$ -CDd particles appeared as multilamellar aggregates exhibiting a striking onion-like organization of densely packed layers that is similar to that observed in phospholipids,<sup>28</sup> mixtures of diglycerol monooleate/glycerol dioleate,<sup>29</sup> and monolinolein/water systems.<sup>30</sup> Different types of organization seem to coexist. Figure 5c shows a particle entirely constituted of concentric layers, whereas that in Figure 5d has an overall hexagonal shape, with concentric layers surrounding a core with lattice fringes suggesting a crystal-like structure. Most particles apply to the second case, albeit with a shape that is generally more spherical than polygonal, and exhibit a hybrid core-shell structure.

The periodicity of the concentric rings in the multilayer structure has been estimated using Fourier transforms of selected cryo-TEM images, and a repeat distance of about 4 nm was found. The images in Figure 6 reveal details on the fine structure of the constituting layers.

Starting from the surface of the nanosphere and going inward, an electron-dense layer was found, followed by groups of two close electron-dense layers (Figure 6a). The distance between the first and third layers corresponds to the 4 nm distance measured by Fourier analysis. Figure 6b shows the periphery of a nanosphere where the constituting layers are interrupted. Judging from several images, it seems that the distance between layers 1 and 2, 3, 4, and so on, was slightly larger than that between layers 2 and 3, 4 and 5, and so forth. The respective distances were difficult to measure with precision considering the high level of noise in the images and the possible distortions induced by radiation damage or compression in the embedding film. Small-angle X-ray scattering experiments on similar samples would certainly allow us to measure more precise values.

Taking into account the chemical structure of the  $\beta$ -CDd molecules that mainly substituted in C2 position, their known

dimensions, and their amphiphilic nature, we proposed a tentative model to describe the packing of concentric bilayers in the nanospheres (Figure 6c). The  $\beta$ -CD rings of the molecule would form layers, with a hydrophilic face on the secondary side of the molecule, whereas the acyl chains would form hydrophobic layers, with a lower density and consequently a contrast in the image lower than that of the  $\beta$ -CD layers. The thickness of the hydrophilic  $\beta$ -CD/ $\beta$ -CD region would be a little less than 2 nm, while that of the hydrophobic C10/C10 layer would be slightly larger, the added thicknesses corresponding approximately to the 4 nm repeat distance. These hypotheses are in accordance with theoretical dimensions of the hydrophilic  $\beta$ -CD/ $\beta$ -CD region estimated at 1.6 nm and the hydrophobic C10/C10 layer estimated at 2.3 nm (SYBYL 7.0 software from Tripos, U.S.).

The structure of the crystalline core of the particles could not be determined as lattice images of several projections of the molecular structure would be necessary. Clear lattice images of the core region can be recorded only when it is oriented along crystallographic zone axes. Another reason for the lack of lattice images of the core is that radiation damage may occur more rapidly in the core than in the surrounding concentric layers.

Electron microscopy results showed that modified cyclodextrins obtained by an enzymatic synthesis route are capable to self-assemble and form either matricial or multilayered particles. Keeping in mind that the particles were all prepared using the same nanoprecipitation procedure, it can be argued that the mode of aggregation depends, to a great extent, on the structure of the amphiphilic cyclodextrins involved.  $\beta$ -CD bearing long acyl chains ( $\beta$ -CDd) may have a hydrophilic/hydrophobic balance that promotes self-organization into bilayers. In contrast, the short-chained  $\beta$ -CD ( $\beta$ -CDh) do not form bilayers and precipitated into dense nanoparticles that do not exhibit any regular molecular structure, that is, at the scale of the characterization techniques we used. These results are, to a certain extent, consistent with those found by Cryan et al.<sup>31</sup> These authors mentioned the formation of 100–300 nm bilayer vesicles from solutions of amphiphilic heptakis [2-oligoethyleneglycol]-6-deoxy-6-hexadecylthiol]- $\beta$ -CD (SC16  $\beta$ -CD), whereas the amphiphilic heptakis [2-oligoethyleneglycol]-6-deoxy-6-hexylthiol]- $\beta$ -CD (SC6  $\beta$ -CD) self-assembled into dense nanoparticles without any layer organization.

Further studies are in progress to fully characterize the ultrastructure of these promising colloidal drug carriers. Indeed, due to the different modes of aggregation which lead to various nanosystems, it can be hypothesized that the latest may present different pathways of entrapping and releasing drug molecules.

## Conclusion

The one-step synthesis of  $\beta$ -CD ester makes thermolysin biocatalysis an exciting alternative to the classical chemical approach for the production of modified  $\beta$ -CD-based nanoagregates. Both hexanoate and decanoate derivatives were mainly substituted on the C2 position. While the hexanoate  $\beta$ -CD ester self-organizes into nanospheres presenting a dense matricial structure, the decanoate derivative yields hybrid structures presenting a crystal-like core surrounded by onion-like concentric bilayers, observed for the first time. Further studies are in progress in order to evaluate the ability of these original nanostructures to associate drugs. The use of these newly synthesized  $\beta$ -CD esters to form reservoir-type nanosystems is also under investigation.

## References and Notes

- (1) Biwer, A.; Antranikian, G.; Heinzle, E. *Appl. Microbiol. Biotechnol.* **2002**, *59*, 609–617.
- (2) Davis, M. E.; Brewster, M. E. *Nat. Rev. Drug Discovery* **2004**, *3*, 1023–1035.
- (3) Freudenberg, K.; Cramer, F.; Plieninger, H. Verfahren zur herstellung von einschlussverbindungen physiologisch wirksamer organischer verbindungen. German Patent DE 895,769, 1953.
- (4) Auzély-Velty, R.; Djedaini-Pilard, S.; Désert, S.; Perly, B.; Zemb, T. H. *Langmuir* **2000**, *16*, 3727–3734.
- (5) Ravoo, B. J.; Darcy, R.; Gambadauro, P.; Mallamace, F. *Langmuir* **2002**, *18*, 1945–1948.
- (6) Donohue, R.; Mazzaglia, A.; Ravoo, B. J.; Darcy, R. *Chem. Commun.* **2002**, 2864–2865.
- (7) Ravoo, B. J.; Darcy, R. *Angew. Chem., Int. Ed.* **2000**, *39*, 4324–4326.
- (8) Duchêne, D.; Ponchel, G.; Wouessidjewe, D. *Adv. Drug Delivery Rev.* **1999**, *36*, 29–40.
- (9) Memisoglu, E.; Bochot, A.; Sen, M.; Charon, D.; Duchêne, D.; Hincal, A. A. *J. Pharmacol. Sci.* **2002**, *91* (5), 1214–1224.
- (10) Gèze, A.; Aous, S.; Baussanne, I.; Putaux, J. L.; Defaye, J.; Wouessidjewe, D. *Int. J. Pharm.* **2002**, *242*, 301–305.
- (11) Lamer, V. K.; Dinegar, R. H. *J. Am. Chem. Soc.* **1950**, *72*, 4847–4854.
- (12) Skiba, M.; Wouessidjewe, D.; Puisieux, F.; Duchêne, D.; Gulik, A. *Int. J. Pharm.* **1996**, *142*, 121–124.
- (13) Fessi, H.; Devissaguet, J. P.; Puisieux, F. Procédés de préparation de systèmes colloïdaux dispersibles d'une substance sous forme de nanocapsules. French Patent FR 86184444, 1986.
- (14) Fessi, H.; Puisieux, F.; Devissaguet, J. P.; Ammoury, N.; Benita, S. *Int. J. Pharm.* **1989**, *55*, 25–28.
- (15) Gèze, A.; Putaux, J. L.; Choisnard, L.; Jéhan, P.; Wouessidjewe, D. *J. Microencapsulation* **2004**, *21* (6), 607–613.
- (16) Zhang, P.; Ling, C. C.; Coleman, A.; Parrot-Lopez, H.; Galons, H. *Tetrahedron Lett.* **1991**, *32*, 2769–2770.
- (17) Carrea, G.; Riva, S. *Angew. Chem., Int. Ed.* **2000**, *39*, 2226–2254.
- (18) Gupta, M. N.; Ipsita, R. *Eur. J. Biochem.* **2004**, *271*, 2575–2583.
- (19) Garcia-Junceda, E.; Garcia-Garcia, J. F.; Bastida, A.; Fernandez-Mayoralas, A. *Bioorg. Med. Chem.* **2004**, *12*, 1817–1834.
- (20) Klohr, K. M.; Koch, W.; Klemm, D.; Dicke, R. European Patent EP 1035 135, 2000.
- (21) Akkara, J. A.; Kaplan, D. L.; Ferdinando, F.; Jonathan, D. S. Transesterification of insoluble polysaccharides. U.S. Patent US 6,063,916, May 16, 2000.
- (22) Pattekhan, H. H.; Divakar, S. *Indian J. Chem., Sect. B* **2002**, *41*, 1025–1027.
- (23) Pedersen, N. R.; Kristensen, J. B.; Bauw, G.; Ravoo, B. J.; Darcy, R.; Larsen, K. L.; Pedersen, L. H. *Tetrahedron: Asymmetry* **2005**, *16*, 615–622.
- (24) Provencher, S. W. *Comput. Phys. Commun.* **1982**, *27*, 229–242.
- (25) Durrieu, V.; Gandini, A.; Belcace, M. N.; Blayo, A.; Eiselé, G.; Putaux, J. L. *J. Appl. Polym. Sci.* **2004**, *94* (2), 700–710.
- (26) *The European Pharmacopoeia*, 4th ed.; Council of Europe: Strasbourg, 2002.
- (27) Choisnard, L.; Gèze, A.; Bigan, M.; Putaux, J. L.; Wouessidjewe, D. *J. Pharm. Pharmaceut. Sci.* **2005**, *8*, 593–600.
- (28) Roux, D.; Chenevier, P.; Pott, T.; Navailles, L.; Regev, O.; Monval, O. M. *Curr. Med. Chem.* **2004**, *11*, 169–177.
- (29) Johnsson, M.; Lam, Y.; Barauskas, J.; Tiberg, F. *Langmuir* **2005**, *21* (11), 5159–5165.
- (30) de Campo, L.; Yaghmur, A.; Sagalowicz, L.; Watzke, H.; Glatter, O. *Langmuir* **2004**, *20*, 5254–5261.
- (31) Cryan, S. A.; Donohue, R.; Ravoo, B. J.; Darcy, R.; O'Driscoll, C. M. *J. Drug Delivery Sci. Technol.* **2004**, *14* (1), 57–62.

BM0507655